Quantum synchronization of two coupled cavities with second harmonic generation

Tony E. Lee* and M. C. Cross
Department of Physics, California Institute of Technology, Pasadena, California 91125, USA
(Dated: September 5, 2012)

Synchronization is a phenomenon that appears throughout physics, biology, and chemistry. There has been much work on how synchronization arises in the classical regime. Motivated by current interest in quantum dissipative systems, we investigate whether synchronization can exist in the quantum regime. We consider a pair of cavities with second harmonic generation. In the classical limit, each cavity has a limit cycle solution, in which the photon number oscillates periodically in time. Coupling between the cavities leads to synchronization of the limit cycles. We follow what happens to the synchronization as the system becomes more quantum, by decreasing the photon number. We find that synchronization between the cavities survives deep in the quantum limit when there is much less than one photon in each cavity, because classical correlations are replaced by quantum correlations. Our results can be extended to a wide variety of quantum models.

arXiv:1209.0742v1 [quant-ph] 4 Sep 2012

Introduction. Synchronization refers to the emergence of temporal order among a collection of objects, each of which oscillate periodically in time [1–3]. Without any interaction between them, they would oscillate independently, but the interaction induces them to oscillate in unison. Synchronization occurs in many natural settings, such as neural networks [4], audience applause [5], and menstration [6]. A striking example is when thousands of fireflies flash in unison [2]. Synchronization also occurs in man-made settings such as Josephson junctions [7], nanomechanical resonators [8], optomechanical arrays [9, 10], and trapped ions [11, 12].

There has been much work on how synchronization arises in a group of interacting oscillators. Each member of the group is usually modeled as a nonlinear dynamical system with a limit-cycle solution [1]. A limit cycle means that in steady state, the system variables oscillate periodically in time. An important feature of a limit cycle is that the phase of oscillation is free and can take any value, i.e., it is not locked to the phase of an external drive. Then due to mutual interaction, the limit cycles of different oscillators spontaneously phase-lock with each other. In fact, there can be macroscopic synchronization in an infinite system, and synchronization can be viewed as a nonequilibrium phase transition to temporal order [13–15]. Synchronization is inherently nonequilibrium, because a limit cycle occurs only in the presence of dissipation.

Models of synchronization are usually based on classical equations of motion. Motivated by recent work on quantum nonequilibrium systems [16–19], we are interested in the basic question of whether a *quantum* system can synchronize. Our approach is to use a quantum model that exhibits limit cycles and synchronization in the classical limit, and then see what happens as the system becomes more quantum. As the quantumness increases, one would expect there to be more quantum noise [20], which would inhibit synchronization. On the other hand, there would also be more entanglement between the oscillators, which might enhance synchronization. It is not clear what happens to synchronization deep in the quantum limit.

In this paper, we consider two coupled optical cavities, each with second harmonic generation. The classical limit here corresponds to many photons in the cavities. In the classical limit, each cavity has a limit cycle, in which the photon number oscillates in time [21]. Coupling between the cavities causes the oscillations to synchronize in-phase or anti-phase. We study what happens as the system becomes more quantum by decreasing the number of photons in the cavities. As the system becomes more quantum, the limit cycles become noisier. However, classical correlations between the cavities are replaced by quantum correlations. We find that synchronization survives in the extreme quantum limit when there is much less than one photon in each cavity.

We decided to base our work on second harmonic generation, because it is the simplest quantum model known to have a limit cycle in the classical limit. Our work can be extended to the many other quantum models also known to have limit cycles, such as Jaynes-Cummings cavities [22, 23], optomechanics [24–26], Rydberg atoms [27, 28], quantum dots [29], and single-electron transistors [30].

During preparation of this manuscript, we became aware of Ref. [31], which studies synchronization of optomechanics in the presence of quantum noise. Our work is different, since we are interested in the extreme quan-

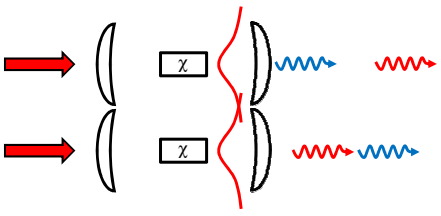

FIG. 1. Two cavities with nonlinear crystals inside are laser-driven and dissipate photons. They are coupled to each other due to overlap of their photonic wavefunctions.

tum limit, when the classical approximation is completely invalid.

Model. In second harmonic generation, a nonlinear crystal within an optical cavity converts light at a fundamental frequency into light at twice the frequency [32]. This setup is widely used for frequency doubling. We extend it to the case of two cavities, each with a nonlinear crystal inside. The cavities are coupled due to overlap of their photonic wavefunctions (Fig. 1). For simplicity, we assume that the cavities are identical.

We first describe the quantum model and then the classical model. Let the two cavities be denoted a and b. Each cavity has two modes: a_1 and a_2 are the annihilation operators for the fundamental and second harmonic modes of the first cavity, while b_1 and b_2 are the corresponding operators for the second cavity. An external laser drives the fundamental mode of both cavities, and the nonlinear crystals produce light at the second harmonic. In the interaction picture and rotating-wave approximation, the Hamiltonian is ($\hbar = 1$)

$$\begin{aligned} H = {} & iE(a_1^\dagger - a_1 + b_1^\dagger - b_1) \\ & + i\frac{\chi}{2}(a_1^{\dagger 2}a_2 - a_1^2 a_2^\dagger + b_1^{\dagger 2}b_2 - b_1^2 b_2^\dagger) \\ & + \Delta_1(a_1^\dagger a_1 + b_1^\dagger b_1) + \Delta_2(a_2^\dagger a_2 + b_2^\dagger b_2) \\ & + V_1(a_1^\dagger b_1 + a_1 b_1^\dagger) + V_2(a_2^\dagger b_2 + a_2 b_2^\dagger), \end{aligned} \tag{1}$$

where E is the laser drive, χ is the second-order susceptibility of the crystal, and Δ_1 and Δ_2 are the frequency detunings of the fundamental and second harmonic from the laser. For generality and to account for possible dispersion, we let Δ_1 and Δ_2 vary independently. The term with χ means that two photons at the fundamental frequency are converted into one photon at the second harmonic; the reverse process is also allowed. V_1 is the coupling between the fundamental modes, and V_2 is the coupling between the second harmonic modes.

Since dissipation is a prerequisite for limit cycles, we let photons leak out of the cavities. The photon decay rates of the fundamental and second harmonic are κ_1 and κ_2, respectively. This open quantum system is described by a Lindblad master equation, which says how the density matrix ρ evolves in time:

$$\begin{aligned} \dot{\rho} = {} & -i[H, \rho] + \sum_{i=1,2} \kappa_i (2a_i \rho a_i^\dagger - a_i^\dagger a_i \rho - \rho a_i^\dagger a_i) \\ & + \sum_{i=1,2} \kappa_i (2b_i \rho b_i^\dagger - b_i^\dagger b_i \rho - \rho b_i^\dagger b_i). \end{aligned} \tag{2}$$

The master equation is linear in ρ and has a unique steady state solution [33].

In the classical approximation to Eq. (2), one assumes that each mode is in a coherent state and that there is no entanglement between the modes [34]. One replaces the operators a_1, a_2, b_1, b_2 with complex numbers that denote the coherent states, $\alpha_1, \alpha_2, \beta_1, \beta_2$. This leads to classical equations of motion that are nonlinear:

$$\dot{\alpha}_1 = E - (\kappa_1 + i\Delta_1)\alpha_1 + \chi \alpha_1^* \alpha_2 - iV_1 \beta_1, \tag{3}$$

$$\dot{\alpha}_2 = \quad -(\kappa_2 + i\Delta_2)\alpha_2 - \frac{\chi}{2}\alpha_1^2 - iV_2 \beta_2, \tag{4}$$

$$\dot{\beta}_1 = E - (\kappa_1 + i\Delta_1)\beta_1 + \chi \beta_1^* \beta_2 - iV_1 \alpha_1, \tag{5}$$

$$\dot{\beta}_2 = \quad -(\kappa_2 + i\Delta_2)\beta_2 - \frac{\chi}{2}\beta_1^2 - iV_2 \alpha_2. \tag{6}$$

In the classical model, the average number of photons in mode a_1 is $\langle a_1^\dagger a_1 \rangle = |\alpha_1|^2$ and similarly for other modes. The classical approximation is an accurate description of the quantum model when there are many photons in each mode [34]. (This occurs when the laser drive is much stronger than the dissipation, since the photon number is determined by the balance of driving and dissipation.) Intuitively, this is because when a mode is highly populated in steady state, it continuously emits photons, so an individual photon emission has negligible effect.

To clarify when the classical model is reliable, it is insightful to rewrite Eqs. (3)–(6) using scaled variables ($\tilde{\alpha}_i = \chi \alpha_i$, $\tilde{\beta}_i = \chi \beta_i$) and scaled parameters ($\tilde{E} = E\chi$). The equations of motion become

$$\dot{\tilde{\alpha}}_1 = \tilde{E} - (\kappa_1 + i\Delta_1)\tilde{\alpha}_1 + \tilde{\alpha}_1^* \tilde{\alpha}_2 - iV_1 \tilde{\beta}_1, \tag{7}$$

$$\dot{\tilde{\alpha}}_2 = \quad -(\kappa_2 + i\Delta_2)\tilde{\alpha}_2 - \frac{1}{2}\tilde{\alpha}_1^2 - iV_2 \tilde{\beta}_2, \tag{8}$$

$$\dot{\tilde{\beta}}_1 = \tilde{E} - (\kappa_1 + i\Delta_1)\tilde{\beta}_1 + \tilde{\beta}_1^* \tilde{\beta}_2 - iV_1 \tilde{\alpha}_1, \tag{9}$$

$$\dot{\tilde{\beta}}_2 = \quad -(\kappa_2 + i\Delta_2)\tilde{\beta}_2 - \frac{1}{2}\tilde{\beta}_1^2 - iV_2 \tilde{\alpha}_2. \tag{10}$$

Since Eqs. (7)–(10) are identical to Eqs. (3)–(6), if we vary E and χ while keeping $E\chi$ constant, the classical dynamics are invariant up to a scaling of α_i and β_i. This provides a controlled way of following the classical-to-quantum transition [34]. We will solve the quantum model while decreasing E and increasing χ, keeping $E\chi$ fixed, so that the photon numbers decrease, e.g., $|\alpha_1|^2 \sim |\tilde{\alpha}_1|^2/\chi^2$. Since the classical dynamics remain the same in this procedure, *any change in behavior must be due to quantum effects.* Thus, the classical limit corresponds to large E and small χ. The quantum limit corresponds to small E and large χ, which makes sense since a weak laser drive results in a small photon number.

To characterize the temporal correlations between the various modes, we calculate:

$$g_2(a_1, a_2) = \frac{\langle a_1^\dagger a_1 a_2^\dagger a_2 \rangle}{\langle a_1^\dagger a_1 \rangle \langle a_2^\dagger a_2 \rangle}, \quad g_2(a_i, b_i) = \frac{\langle a_i^\dagger a_i b_i^\dagger b_i \rangle}{\langle a_i^\dagger a_i \rangle \langle b_i^\dagger b_i \rangle}. \tag{11}$$

When $g_2 > 1$, the two modes are positively correlated and tend to emit photons simultaneously (bunching). When $g_2 < 1$, they are negatively correlated and tend not to emit simultaneously (antibunching). When $g_2 = 1$, there are no correlations. g_2 is a convenient measure, since it works in both quantum and classical models. In the

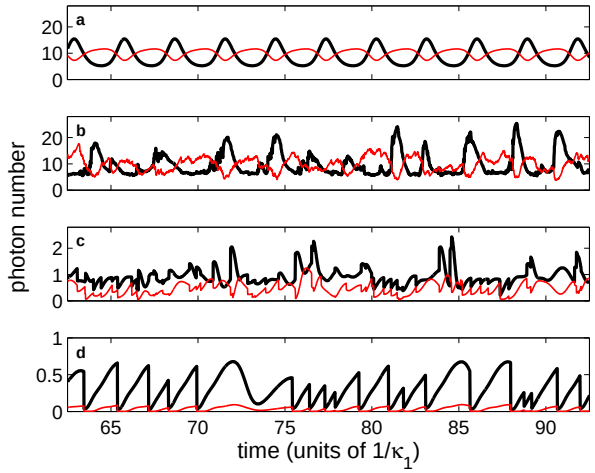

FIG. 2. Classical and quantum trajectories for one cavity, showing photon numbers of mode a_1 (thick, black line) and mode a_2 (thin, red line) over time. (a) Limit-cycle solution of the classical model for $E = 8\kappa_1, \chi = 0.8\kappa_1$. (b)–(d) Quantum trajectories for the same system, but as it becomes more quantum: (b) $E = 8\kappa_1, \chi = 0.8\kappa_1$, (c) $E = 2\kappa_1, \chi = 3.2\kappa_1$, (d) $E = \kappa_1, \chi = 6.4\kappa_1$. All plots use $\kappa_2 = 0.5\kappa_1, \Delta_1 = 0.5\kappa_1, \Delta_2 = \kappa_1$. In (d), the modes are antibunched with each other due to quantum correlations, despite appearing to be positively correlated in the plot.

quantum model, expectation values are taken with respect to the steady state ρ. In the classical model, expectation values are averages over time.

One cavity, classical model. Here we review the results of the classical model for one cavity, i.e., Eqs. (3) and (4) with $V_1 = V_2 = 0$. Suppose one increases E while keeping the other parameters constant. At a critical value E_c, a Hopf bifurcation occurs [21]. When $E < E_c$, the system has a stable fixed point solution, $\alpha_1(t) = \bar{\alpha}_1$ and $\alpha_2(t) = \bar{\alpha}_2$, so the photon numbers are constant in steady state. When E crosses E_c, the fixed point becomes unstable, and a stable limit cycle appears. In this limit cycle solution, α_1 and α_2 oscillate periodically in time, and as a result, the photon numbers $|\alpha_1|^2$ and $|\alpha_2|^2$ also oscillate [Fig. 2(a)]. As E increases further, the oscillations increase in amplitude and become nonsinusoidal. E_c is a complicated function of χ, κ_i, Δ_i.

The existence of the limit cycle can be intuitively understood as follows. When E is small, α_1 and α_2 are small, so the nonlinear terms proportional to χ in Eqs. (3) and (4) have negligible effect. But for sufficiently large E, α_1 and α_2 are large, and the χ terms dominate. The effect of the χ terms is to exchange energy back and forth between the two modes. This exchange is seen in Fig. 2(a), where $|\alpha_1|^2$ and $|\alpha_2|^2$ are roughly anti-phase with each other.

The temporal correlations between $|\alpha_1|^2$ and $|\alpha_2|^2$ are captured by $g_2(a_1, a_2)$. When $E < E_c$, there are no correlations: $g_2(a_1, a_2) = 1$. When $E > E_c$, the modes are negatively correlated: $g_2(a_1, a_2) < 1$. Thus, $g_2(a_1, a_2)$ is an indicator of the existence of the limit cycle. Note that the correlations are completely *classical*.

Although $|\alpha_1|^2$ and $|\alpha_2|^2$ oscillate together, they are not said to be "synchronized," since they belong to the same limit cycle. Also, it is important to note that the limit cycle's phase of oscillation is free and not fixed to the phase of the laser drive; this allows two oscillators to *spontaneously* synchronize with each other [1].

Two cavities, classical model. Now we study the synchronization of two cavities in the classical limit. Following convention, we assume that the coupling V_i is small, so that the limit cycle of each cavity remains well-defined and retains its identity in the presence of coupling [1].

To identify the steady state solutions of the coupled system, it is useful to reduce Eqs. (3)–(6) to the normal form of a Hopf bifurcation [35]. This means to expand the equations perturbatively in $E - E_c$ and V_i. Again, let the fixed point solution of one cavity in the absence of coupling be $\bar{\alpha}_1$ and $\bar{\alpha}_2$, which depend on $E, \chi, \kappa_i, \Delta_i$. Let $\vec{x}$ and $\vec{y}$ be deviations each cavity from the fixed point:

$$\vec{x} = \begin{pmatrix} \mathrm{Re}(\alpha_1 - \bar{\alpha}_1) \\ \mathrm{Im}(\alpha_1 - \bar{\alpha}_1) \\ \mathrm{Re}(\alpha_2 - \bar{\alpha}_2) \\ \mathrm{Im}(\alpha_2 - \bar{\alpha}_2) \end{pmatrix}, \quad \vec{y} = \begin{pmatrix} \mathrm{Re}(\beta_1 - \bar{\alpha}_1) \\ \mathrm{Im}(\beta_1 - \bar{\alpha}_1) \\ \mathrm{Re}(\beta_2 - \bar{\alpha}_2) \\ \mathrm{Im}(\beta_2 - \bar{\alpha}_2) \end{pmatrix}. \quad (12)$$

Then $\vec{x} = z_a(t)\vec{p} + z_a(t)^*\vec{p}^*$ and $\vec{y} = z_b(t)\vec{p} + z_b(t)^*\vec{p}^*$, where $\vec{p}$ is the eigenvector of the linearized system that becomes unstable at E_c. $z_a(t)$ and $z_b(t)$ are the complex amplitudes for each cavity, and they obey

$$\frac{dz_a}{dt} = (h_1 + ih_2)z_a + (h_3 + ih_4)|z_a|^2 z_a + (h_5 + ih_6)z_b, \quad (13)$$

$$\frac{dz_b}{dt} = (h_1 + ih_2)z_b + (h_3 + ih_4)|z_b|^2 z_b + (h_5 + ih_6)z_a, \quad (14)$$

where h_i depends on the original parameters.

We are interested in the steady states of Eqs. (13) and (14). The two most important steady state solutions are $z_a(t) = -z_b(t) = c_1 e^{i\Omega_1 t}$ and $z_a(t) = z_b(t) = c_2 e^{i\Omega_2 t}$, where $c_1, c_2, \Omega_1, \Omega_2$ are constants. The first solution means that $|\alpha_1|^2$ oscillates anti-phase with $|\beta_1|^2$, and $|\alpha_2|^2$ oscillates anti-phase with $|\beta_2|^2$ [Fig. 3(a)]. The second solution means that $|\alpha_1|^2$ oscillates in-phase with $|\beta_1|^2$, and $|\alpha_2|^2$ oscillates in-phase with $|\beta_2|^2$ [Fig. 3(b)]. Which solution is stable depends on the parameters. The phase diagram is shown in Fig. 4(a).

Equations (13) and (14) have other steady state solutions. However, in the limit of small coupling, only the two above solutions exist. This is a well-known result found by rewriting the equations in terms of amplitudes and phases and then adiabatically eliminating the amplitudes to obtain a phase equation [1]. Hence, we limit

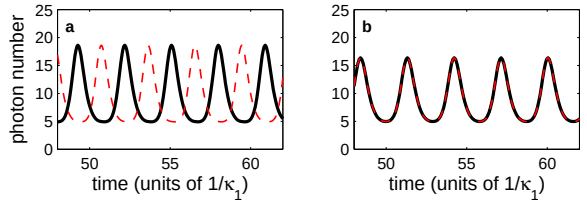

FIG. 3. Steady state solutions of the classical model for two coupled cavities. Photon numbers of mode a_1 (solid, black line) and mode b_1 (dashed, red line) are plotted. (a) Anti-phase synchrony for $\Delta_1 = 0.5\kappa_1, \Delta_2 = \kappa_1$. (b) In-phase synchrony for $\Delta_1 = -0.5\kappa_1, \Delta_2 = -\kappa_1$. Both plots use: $E = 8\kappa_1, \chi = 0.8\kappa_1, \kappa_2 = 0.5\kappa_1, V_1 = 0.1\kappa_1, V_2 = 0$.

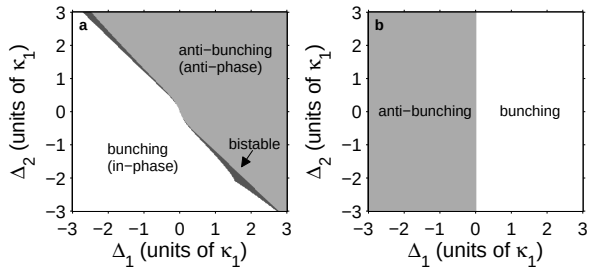

FIG. 4. Phase diagram for two coupled cavities as a function of Δ_1 and Δ_2, showing when a_1 and b_1 are bunched or anti-bunched. (a) Classical limit, showing in-phase or anti-phase synchrony. There is sometimes bistability between the two solutions. The parameters are $\chi = 0.8\kappa_1, \kappa_2 = 0.5\kappa_1, V_1 = 0.05\kappa_1, V_2 = 0$. For each value of Δ_1 and Δ_2, E is set to $E_c + 0.5\kappa_1$. (b) Extreme quantum limit for the same parameters, except with $E \to 0$ and $\chi \to \infty$.

our discussion to the in-phase and anti-phase solutions. (The solutions for general coupling have been discussed for the cases of $h_5 = 0$ [12] and $h_6 = 0$ [36].)

Thus, although the coupling is weak, the cavities synchronize with each other. When the synchronization is in-phase, $g_2(a_1, b_1), g_2(a_2, b_2) > 1$. When the synchronization is anti-phase, $g_2(a_1, b_1), g_2(a_2, b_2) < 1$. Again, these correlations are classical.

One cavity, quantum model. Now we consider what happens with one cavity in the quantum limit. Figures 2(b)–(d) show simulations of the quantum model, generated using the method of quantum trajectories [37, 38]. Clearly, as the system becomes more quantum, the limit cycle becomes noisier, since the classical approximation is less accurate [20]. (A single photon emission has more effect on the wavefunction when there are fewer photons overall.) In the extreme quantum limit, when there is much less than one photon in each mode, the limit cycle is not visually identifiable at all [Fig. 2(d)]. One might think that the correlations between a_1 and a_2 have disappeared. On the contrary, the correlations are strong but now quantum in nature.

To find these quantum correlations in the extreme

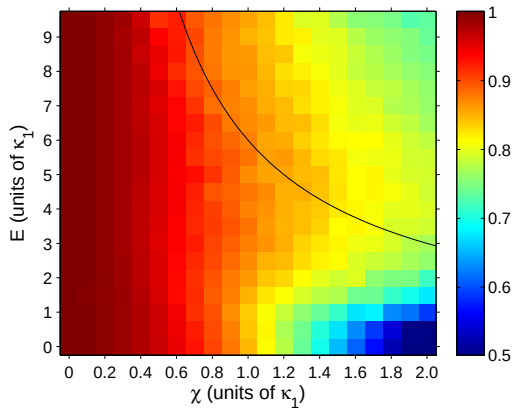

FIG. 5. The correlation $g_2(a_1, a_2)$ for one cavity, plotted as a function of E and χ, using color scale on right. The black line indicates the location of the Hopf bifurcation E_c as a function of χ. Parameters are $\kappa_2 = 0.5\kappa_1$, $\Delta_1 = 0.5\kappa_1$, $\Delta_2 = \kappa_1$. This plot was generated using the quantum trajectory method, so there is some noise due to statistical uncertainty.

quantum limit, we analytically solve for the steady state ρ of Eq. (2) in a perturbation series of E. By doing this to sixth order in E, we find $g_2(a_1, a_2)$ to first order in E:

$$g_2(a_1, a_2) = \frac{1}{1 + \frac{\frac{1}{4}\chi^4 + \chi^2[-\Delta_1(\Delta_1+\Delta_2) + \kappa_1(\kappa_1+\kappa_2)]}{(\Delta_1^2+\kappa_1^2)[(\Delta_1+\Delta_2)^2+(\kappa_1+\kappa_2)^2]}} + O(E^2). \tag{15}$$

Recall that the quantum limit corresponds to $E \to 0$ and $\chi \to \infty$. Thus, in the extreme quantum limit, $g_2(a_1, a_2) = 0$, i.e., there is strong antibunching between a_1 and a_2. This result is independent of κ_i, Δ_i.

Figure 5 shows the classical-to-quantum transition. In the classical limit, $g_2(a_1, a_2) = 1$ when $E < E_c$ and $g_2(a_1, a_2) < 1$ when $E > E_c$, where E_c is the location of the Hopf bifurcation. As the system becomes more quantum, the transition at E_c smoothes out, and the region of antibunching expands into $E < E_c$. Also, antibunching in the classical limit gradually develops into strong antibunching in the quantum limit. In this sense, the two modes still exchange energy back and forth, but the correlations are now quantum instead of classical. In the extreme quantum limit, the classical approximation is completely wrong, demonstrating the presence of quantum correlations. In fact, the presence of entanglement is clearly seen in Fig. 2(d): when one mode decays, the other one instantaneously changes.

Two cavities, quantum model. Finally, we consider the synchronization of two cavities in the quantum limit. Recall that in the classical limit, the cavities were in-phase $[g_2(a_1, b_1) > 1]$ or anti-phase $[g_2(a_1, b_1) < 1]$ with each other, depending on the parameters. We want to see what happens to these correlations in the extreme quantum limit. In classical systems, noise inhibits synchronization because it causes the phases of the oscillators

to drift with respect to each other [1]. Hence, one would expect quantum noise to wash away any trace of synchronization between the oscillators.

To find $g_2(a_1, b_1)$ in the quantum limit, we again solve Eq. (2) in a perturbation series of E but now include V_1 and V_2. By solving for the steady state ρ to fourth order in E, we obtain an analytical expression for $g_2(a_1, b_1)$ to first order in E. In the limit of $\chi \to \infty$,

$$g_2(a_1, b_1) = \frac{\kappa_1^2 + (\Delta_1 + V_1)^2}{\kappa_1^2 + \Delta_1^2} + O(E^2), \qquad (16)$$

which is independent of Δ_2, κ_2, V_2. For small V_1,

$$g_2(a_1, b_1) \approx 1 + \frac{2\Delta_1 V_1}{\kappa_1^2 + \Delta_1^2}. \qquad (17)$$

Whether a_1 and b_1 are bunched or antibunched depends on the sign of $\Delta_1 V_1$. The phase diagram is shown in Fig. 4(b). (Numerically, we find that the phase diagram for a_2 and b_2 is very similar.) The fact that the phase diagram is different from the classical result in Fig. 4(a) demonstrates the importance of quantum correlations in the quantum limit.

Equation (17) shows that even in the extreme quantum limit, there are significant correlations between a_1 and b_1. So despite the presence of much quantum noise, synchronization survives because classical correlations are replaced by quantum correlations. Note that while one might expect some sort of correlation for finite E and χ, it is not obvious that the correlations would still exist in the limit of $E \to 0$ and $\chi \to \infty$.

Conclusion. We have shown that synchronization survives deep in the quantum limit. Our result raises the question of whether a macroscopic number of oscillators can also synchronize in the quantum limit. Classical synchronizing systems are known to exhibit phase transitions and scaling behavior similar to equilibrium systems [39, 40]. One should investigate how quantum fluctuations affect these critical properties.

It would be interesting to study quantum synchronization using the other quantum models known to exhibit limit cycles, as discussed in the introduction. A promising approach is to use coupled cavities with Jaynes-Cummings nonlinearity [18, 41], since one can fabricate a large of array of such cavities in the microwave regime [42]. Perhaps synchronization is as widespread in the quantum regime as it is in the classical regime.

We thank Mark Rudner for useful discussions. This work was supported by NSF Grant No. DMR-1003337.

* Current address: ITAMP, Harvard-Smithsonian Center for Astrophysics, Cambridge, MA 02138, USA; e-mail: tonylee@cfa.harvard.edu

[1] A. S. Pikovsky, M. Rosenblum, and J. Kurths, *Synchronization: A Universal Concept in Nonlinear Science* (Cambridge University Press, New York, 2001).
[2] S. H. Strogatz, *Sync: The Emerging Science of Spontaneous Order* (Hyperion, New York, 2003).
[3] J. A. Acebrón, L. L. Bonilla, C. J. Pérez Vicente, F. Ritort, and R. Spigler, Rev. Mod. Phys. **77**, 137 (2005).
[4] F. Varela, J.-P. Lachaux, E. Rodriguez, and J. Martinerie, Nat. Rev. Neurosci. **2**, 229 (2001).
[5] Z. Néda, E. Ravasz, Y. Brechet, T. Vicsek, and A. L. Barabási, Nature **403**, 849 (2000).
[6] M. K. McClintock, Nature **229**, 244 (1971).
[7] K. Wiesenfeld, P. Colet, and S. H. Strogatz, Phys. Rev. Lett. **76**, 404 (1996).
[8] M. C. Cross, A. Zumdieck, R. Lifshitz, and J. L. Rogers, Phys. Rev. Lett. **93**, 224101 (2004).
[9] G. Heinrich, M. Ludwig, J. Qian, B. Kubala, and F. Marquardt, Phys. Rev. Lett. **107**, 043603 (2011).
[10] C. A. Holmes, C. P. Meaney, and G. J. Milburn, Phys. Rev. E **85**, 066203 (2012).
[11] S. Knünz, M. Herrmann, V. Batteiger, G. Saathoff, T. W. Hänsch, K. Vahala, and T. Udem, Phys. Rev. Lett. **105**, 013004 (2010).
[12] T. E. Lee and M. C. Cross, Phys. Rev. Lett. **106**, 143001 (2011).
[13] H. Sakaguchi, S. Shinomoto, and Y. Kuramoto, Prog. Theor. Phys. **77**, 1005 (1987).
[14] S. H. Strogatz and R. E. Mirollo, J. Phys. A **21**, L699 (1988).
[15] H. Daido, Phys. Rev. Lett. **61**, 231 (1988).
[16] S. Diehl, A. Micheli, A. Kantian, B. Kraus, H. Büchler, and P. Zoller, Nature Physics **4**, 878 (2008).
[17] M. S. Rudner and L. S. Levitov, Phys. Rev. Lett. **102**, 065703 (2009).
[18] F. Nissen, S. Schmidt, M. Biondi, G. Blatter, H. E. Türeci, and J. Keeling, Phys. Rev. Lett. **108**, 233603 (2012).
[19] B. Olmos, I. Lesanovsky, and J. P. Garrahan, Phys. Rev. Lett. **109**, 020403 (2012).
[20] C. M. Savage, Phys. Rev. A **37**, 158 (1988).
[21] P. D. Drummond, K. J. McNeil, and D. F. Walls, Optica Acta **27**, 321 (1980).
[22] H. Gang, C.-Z. Ning, and H. Haken, Phys. Rev. A **41**, 2702 (1990).
[23] M. A. Armen and H. Mabuchi, Phys. Rev. A **73**, 063801 (2006).
[24] T. J. Kippenberg, H. Rokhsari, T. Carmon, A. Scherer, and K. J. Vahala, Phys. Rev. Lett. **95**, 033901 (2005).
[25] F. Marquardt, J. G. E. Harris, and S. M. Girvin, Phys. Rev. Lett. **96**, 103901 (2006).
[26] M. Ludwig, B. Kubala, and F. Marquardt, New J. Phys. **10**, 095013 (2008).
[27] T. E. Lee, H. Häffner, and M. C. Cross, Phys. Rev. A **84**, 031402 (2011).
[28] J. Qian, G. Dong, L. Zhou, and W. Zhang, Phys. Rev. A **85**, 065401 (2012).
[29] K. Ono and S. Tarucha, Phys. Rev. Lett. **92**, 256803 (2004).
[30] D. A. Rodrigues, J. Imbers, and A. D. Armour, Phys. Rev. Lett. **98**, 067204 (2007).
[31] M. Ludwig and F. Marquardt, arXiv:1208.0327.
[32] P. A. Franken, A. E. Hill, C. W. Peters, and G. Weinreich, Phys. Rev. Lett. **7**, 118 (1961).
[33] S. G. Schirmer and X. Wang, Phys. Rev. A **81**, 062306

(2010).
[34] X. Zheng and C. M. Savage, Phys. Rev. A **51**, 792 (1995).
[35] A. H. Nayfeh, *Method of Normal Forms* (Wiley, New York, 1993).
[36] D. Aronson, G. Ermentrout, and N. Kopell, Physica D **41**, 403 (1990).
[37] J. Dalibard, Y. Castin, and K. Mølmer, Phys. Rev. Lett. **68**, 580 (1992).
[38] R. Dum, P. Zoller, and H. Ritsch, Phys. Rev. A **45**, 4879 (1992).
[39] H. Hong, H. Park, and M. Y. Choi, Phys. Rev. E **72**, 036217 (2005).
[40] T. E. Lee, G. Refael, M. C. Cross, O. Kogan, and J. L. Rogers, Phys. Rev. E **80**, 046210 (2009).
[41] J. Koch, A. A. Houck, K. L. Hur, and S. M. Girvin, Phys. Rev. A **82**, 043811 (2010).
[42] D. L. Underwood, W. E. Shanks, J. Koch, and A. A. Houck, Phys. Rev. A **86**, 023837 (2012).